Research Square

Preprints are preliminary reports that have not undergone peer review.
They should not be considered conclusive, used to inform clinical practice,
or referenced by the media as validated information.

Metabolic profiles and correlation with surgical outcomes in mesial versus neocortical temporal lobe epilepsy

Haoyue Zhu
Xiangya Hospital Central South University
Yongxiang Tang
Xiangya Hospital Central South University
Ling Xiao
Xiangya Hospital Central South University
Shirui Wen
Xiangya Hospital Central South University
Yuanxia Wu
Xiangya Hospital Central South University
Zhiquan Yang
Xiangya Hospital Central South University
Luo Zhou
Xiangya Hospital Central South University
Bo Xiao
Xiangya Hospital Central South University
Li Feng
Xiangya Hospital Central South University
Shuo Hu (hushuo2018@163.com)
Xiangya Hospital Central South University https://orcid.org/0000-0003-0998-8943

Research Article

Keywords: 18F-FDG-PET, MTLE, NTLE, Metabolic profile, Surgical prognosis

Posted Date: June 9th, 2022

DOI: https://doi.org/10.21203/rs.3.rs-1673079/v1

License: This work is licensed under a Creative Commons Attribution 4.0 International License. Read Full License

Abstract

Purpose Differentiating mesial temporal lobe epilepsy (MTLE) and neocortical temporal lobe epilepsy (NTLE) remains a challenge. Our study aimed at characterization of the metabolic profiles between MTLE and NTLE, as well as their correlation with surgical prognosis by using ^{18}F-FDG-PET.

Methods In total, 137 patients with intractable TLE and 40 age-matched healthy controls were recruited. Patients were divided into MTLE group (N = 91) and NTLE group (N = 46). ^{18}F-FDG-PET was used to measure the metabolism of regional cerebra, which was analyzed by statistical parametric mapping. The volume of abnormal metabolism in cerebral regions and their relationship with surgical prognosis were calculated for each surgical patient.

Results The cerebral hypometabolism of MTLE is limited to the ipsilateral temporal and insular lobes ($p<0.001$, uncorrected), while the NTLE patients showed hypometabolism in the ipsilateral temporal, frontal and parietal lobes ($p<0.001$, uncorrected). The MTLE patients showed extensive hypermetabolism in cerebral regions ($p<0.001$, uncorrected). Hypermetabolism in NTLE is limited to contralateral temporal lobe and cerebellum, ipsilateral frontal, occipital lobe, and bilateral thalamus ($p<0.001$, uncorrected). Among patients who underwent resection of epileptic lesions, 51 (67.1%) patients in the MTLE group and 10 (43.5%) in NTLE achieved an Engel class IA outcome ($p=0.041$). In the MTLE group, the volumes of metabolic increase for frontal lobe or thalamus were larger in non-Engel class IA patients than in Engel class IA patients ($p<0.05$).

Conclusion Spatial metabolic profile could discriminate NTLE from MTLE. In MTLE, hypermetabolism of thalamus and frontal lobe could facilitate preoperative counseling and surgical planning.

Introduction

Approximately 40% of patients with temporal lobe epilepsy (TLE) develop drug-resistant epilepsy that may require surgical treatment[1]. Classified by the epileptogenic area, two main syndromes have been described in TLE, which are mesial temporal epilepsy (MTLE) and neocortical temporal epilepsy (NTLE)[2]. A standardized anterior temporal lobectomy is the most targeted and efficient procedure for the treatment of MTLE[3], whereas the tailored resection of the lateral temporal neocortex is often chosen for NTLE[4]. However, the postoperative seizure outcome is not as favorable in NTLE as in MTLE[5]. Further improvements such as precise identification of TLE subtypes and localization of epileptogenic zone (EZ) should allow elaborating tailored surgical strategies for each patient in order to achieve better seizure outcome.

The classification of the TLE subtype is based on seizure symptomatology, ictal and interictal scalp electroencephalography (EEG), as well as structural magnetic resonance imaging (MRI). But the majority of patients with MTLE or NTLE share similar clinical pictures, including viscerosensory aura, behavioral arrest, automatism, impaired consciousness, or secondary bilateral tonic-clonic seizures[6]. They also demonstrated similar patterns of EEG recordings showing episodic spikes and/or slow waves localized over unilateral temporal region interictally[4, 7]. In the case of TLE with MRI-invisible lesions, it would be much more difficult to differentiate NTLE from MTLE on the basis of structural brain imaging[5]. The use of preoperative high-resolution morphometric MRI or molecular imaging may help discriminate the subtypes of TLE patients and localize the region of seizure origination to improve surgical results via optimized presurgical planning.

Fluorine-18-fluorodeoxyglucose-positron emission tomography (^{18}F-FDG-PET) has been well accepted as an irreplaceable noninvasive presurgical molecular imaging method for patients with TLE[8]. ^{18}F-FDG, as a sensitive in vivo imaging trace, has been widely applied to reveal focal hypometabolic regions concordant with seizure onset[9]. PET hypometabolism is proposed as a promising indicator for presurgical evaluation of postoperative outcomes in drug-resistant TLE patients[10]. In-depth evaluation combined with semiology, EEG findings, structural MRI, and PET would further improve EZ localization accuracy and postsurgical prediction in refractory epilepsy[11–15]. In neurodegenerative diseases with dementia, ^{18}F-FDG-PET reveals lobar-specific patterns of hypometabolism related to particular types of dementia. For example, in Alzheimer's disease, ^{18}F-FDG-PET/computed tomography (CT) shows that hypometabolism first appears in the precuneus and posterior cingulate cortex, then in the temporoparietal lobes[16], while hypometabolism in frontal and anterior temporal lobes with later involvement of the parietal lobes is more suggestive of frontotemporal dementia[17]. We infer that MTLE and NTLE may also have different glucose metabolic features which would assist the classification of TLE subtypes and surgical evaluation of outcomes.

In our study, we retrospectively analyzed patients with TLE and reviewed their clinical, neuroelectrophysiological, neuroimaging, surgical, and follow-up data. The patients were then categorized into MTLE and NTLE subgroups to screen interictal whole-brain voxel-based metabolic profiles by ^{18}F-FDG-PET using statistical parametric mapping (SPM12) analysis. The correlation of different glucose metabolic levels was performed with surgical outcomes separately to investigate the underlying neural network and guide the planning of procedures.

Materials And Methods

Study participants and clinical assessments

From January 2016 to June 2021, we recruited 137 patients with intractable TLE and 40 age-matched healthy controls (HC) at Xiangya Hospital, Central South University. Patients were diagnosed and classified on the basis of the 2017 International League Against Epilepsy (ILAE) classification of seizure types[18, 19]. We collected the history, seizure symptoms, MRI, video EEG, and invasive stereo-EEG (SEEG) recording of all patients, as well as surgery data and outcomes of patients who underwent epilepsy surgery. The prognostication of the outcome was graded according to the Engel Surgical Outcome scale[20, 21]. Patients with a history of severe systemic or psychiatric illness, drug abuse, and substance use disorder were excluded. The lateralization and localization of EZ and therapy were determined by a multidisciplinary team (MDT) consisting of two experienced epileptologists, a neuroelectrophysiologist, a neuroradiologist, and two neurosurgeons. According to these comprehensive data, patients were categorized into MTLE group and NTLE group. ^{18}F-FDG-PET was used to measure the metabolism of regional cerebral of all patients. The Institutional Review Committee of Xiangya Hospital approved the protocol before patient recruitment commenced. All participants provided informed consent in writing before participation. For participants under the age of 16 years, consents were obtained from their legal guardians.

^{18} F-FDG-PET image examination

Within one week of clinical evaluation, ^{18}F-FDG-PET scanning was done by a Discovery Elite PET/CT scanner (GE Healthcare, Boston, MA, USA). Antiseizure medications (ASMs) were discontinued for at least 24 hours and patients were fasted for at least 6 hours before ^{18}F-FDG injection. Under strict surveillance, patients were confirmed to have no clinically visible seizures within 24 hours and would have a continuous EEG recording 2 hours before tracer injection to ensure that ^{18}F-FDG is not implemented in a post-ictal situation[22]. The ^{18}F-FDG was injected intravenously through the cubital vein at a dose of 3.7 MBq/kg over one minute. Static PET/CT images were acquired in three dimensions over 60 minutes after tracer injection. Participants were laid flat in the PET scanner allowing slices were parallel to the canthomeatal line. The full width of the scan at half maximum was 5.4 mm. The detailed protocol of PET scan has been described previously[23].

Data analyses

The SPM12 (Wellcome Department of Cognitive Neurology, UK) implemented on MATLAB was used to perform image processing. The spatial standard of individual ^{18}F-FDG-PET image volumes was normalized into Montreal Neurological Institute (MNI) space with 2×2×2 voxel sizes. We used an 8-mm full-width-half-maximum Gaussian kernel to blur individual variations in the rotative anatomy and to improve within-participant spatial alignment, then smoothed data for statistical analysis. Given that different lateralities of seizure onset may confuse data, we compared cerebral metabolism of patients with MTLE on the left and right side, as well as patients with NTLE on the left and right side separately against HC. A general linear model was used to administrate voxel-by-voxel univariate statistical tests.

Metabolic alterations were obtained at an uncorrected height threshold (significance of voxel-level) of $p < 0.001$, with cluster size (K_E) above 20 contiguous voxels. After SPM12 preprocessing, xjView toolkits (http://www.alivelearn.net/xjview) were used to visualize, report, and label anatomically the significant clusters. Data of metabolic pattern information about the clusters were obtained, including the number of voxels, peak intensity of each cluster, and anatomical location, which used Automated Anatomical Labeling (AAL) to approximate Brodmann areas.

Statistical Analyses

The statistical analyses were performed using SPSS software for Windows (IBM SPSS Statistics, Version 26.0). Continuous variables were summarized as mean ± standard deviation (SD) or median (interquartile range, IQR). Mann-Whitney U test or Student's t-test was used for comparisons of quantitative variables between MTLE and NTLE groups, as well as all patients and HC. The Chi-square test or Fisher's test was used for qualitative variables. All statistical tests were two-sided, and $p < 0.05$ indicated statistical significance.

For PET image analysis, Analysis of covariance (ANCOVA) was used to compare baseline glucose uptake values of each epilepsy group (left and right MTLE, then left and right NTLE) and HC, with the group as the between-subject factor and age and sex as confounding covariates. A two-sample t-test was used to compare the different groups. Metabolic changes in the whole brain and cerebellum were then calculated, comparing MTLE and NTLE groups to HC separately. Finally, the volumes of metabolic changes, including hypermetabolism and hypometabolism, in temporal and extratemporal areas and their relationship with surgical prognosis for each surgical patient were also calculated.

Results

Demographic and clinical characteristics

There were 91 MTLE (56 men and 35 women; mean age 23.11 ± 7.33 years) and 46 NTLE patients (28 men and 18 women; mean age 19.78 ± 10.82 years, Table 1) included in this study. The mean age for all patients was 22.99 ± 8.76 years. 40 volunteers (21 men and 19 women; mean age 21.60 ± 8.44 years) were recruited as HC. For the clinical characteristics, there were no significant differences in onset age (13.43 ± 7.17

years in MTLE vs. 11.92 ± 9.33 years in NTLE), duration of epilepsy (9.67 ± 6.90 years in MTLE vs. 7.86 ± 6.16 years in NTLE), frequency of seizures and lateralization distribution between two subgroups. Thereinto, 12 (13.2%) patients in MTLE group and 13 (28.3%) patients in NTLE group underwent SEEG monitoring. The demographic and clinical characteristics of the participants are summarized in Tables 1

Table 1
Demographics of participants and clinical characteristics of patients.

	MTLE(N = 91)	NTLE(N = 46)	P value	Total patients(N = 137)	HC(N = 40)	P value
Age (mean ± SD)	23.11 ± 7.33	19.78 ± 10.82	0.065[&]	22.99 ± 8.76	21.60 ± 8.44	0.802[&]
Sex						
Male, n (%)	56(61.5%)	28(60.9%)	0.939[#]	84(61.3%)	21(52.5%)	0.318[#]
Female, n (%)	35(38.5%)	18(39.1)		53(38.7)	19(47.5%)	
Onset age (mean ± SD), year	13.43 ± 7.17	11.92 ± 9.33	0.300[&]	12.93 ± 7.96	-	NA
Duration of epilepsy (mean ± SD), year	9.67 ± 6.90	7.86 ± 6.16	0.135[&]	9.07 ± 6.69	-	NA
Frequency of seizure, n (%)						
<once half a year	6(6.6%)	2(4.4%)	0.207[ε]	8(5.8%)	-	NA
<once a month	8(8.8%)	7(15.2%)		15(10.9%)	-	NA
≥once a month	57(62.6%)	19(41.3%)		76(55.5%)	-	NA
Daily	20(22.0%)	18(39.1%)		38(27.7%)	-	NA
SEEG, n (%)	12(13.2%)	13(28.3%)	0.031[#,*]	25(18.2%)	-	NA
lateralization, n (%)						
Left	48(53.3%)	28(60.9%)	0.402[#]	76(55.5%)	-	NA
Right	43(46.7%)	18(39.1%)		61(44.5%)	-	NA
& Student *t* test						
# Chi-square test or Fisher Exact test						
ε Mann-Whitney *U* test						
* Bold values indicate significant difference (P < 0.05)						
HC, heathy controls; MTLE, mesial temporal lobe epilepsy; NA, not application; NTLE, neocortical temporal lobe epilepsy; SD, standard deviation; SEEG, stereoelectroencephalography.						

Metabolic abnormalities in patients with MTLE

In the MTLE group, the epileptogenic regions were well-lateralized to the left MTLE (n = 46) and right MTLE (n = 43) based on the routine clinical reports with concordant static ^{18}F-FDG-PET hypometabolism. Comparing MTLE to HC, the cerebral hypometabolism of MTLE was limited to the ipsilateral temporal and insular lobe ($p < 0.001$, uncorrected). While extensive changes of cerebral hypermetabolism were present in contralateral temporal, bilateral frontoparietal, occipital regions, limbic lobe, corpus callosum, thalamus, basal ganglia, brainstem, and cerebellum ($p < 0.001$, uncorrected). The affected limbic lobe included the cingulate gyrus, parahippocampal gyrus, and amygdala. The render and slice view of MTLE compared with HC was shown in Fig. 1. Table 2 lists the peaks of the most significant voxels and shows the location of the voxels within each cluster.

Table 2

Location and peaks of significant reduction/increasing in glucose metabolism in patients with MTLE or NTLE compared with heathy controls.

Region	Brodmann Area	Coordinates(mm)			Peak level				Cluster level			
		X	Y	Z	p(FWE-corr)	p(FDR-corr)	T	Z	p(unc)	p(FWE-corr)	K_E	p(unc)
Left MTLE vs Control												
Hippocampus_R (aal3v1)		32	-8	-24	0.000	0.000	6.224	5.639	0.000	0.000	25001	0.000
Fusiform_R (aal3v1)		42	-50	-24	0.000	0.000	6.169	5.598	0.000			
Frontal_Inf_Tri_R (aal3v1)		38	-32	8	0.001	0.000	5.770	5.290	0.000			
Paracentral_Lobule_R (aal3v1)		8	-26	60	0.011	0.000	5.141	4.787	0.000	0.136	249	0.039
Paracentral_Lobule_L (aal3v1)	6	-10	-32	60	0.101	0.001	4.475	4.231	0.000	0.223	189	0.068
Left Frontal Lobe Sub-Gyral		-18	-24	52	0.856	0.003	3.462	3.340	0.000			
Frontal_Inf_Oper_R (aal3v1)		30	8	34	0.187	0.001	4.262	4.048	0.000	0.601	71	0.246
Left Middle Frontal Gyrus		-32	38	-2	0.311	0.001	4.067	3.879	0.000	0.620	67	0.259
Cingulate_Mid_R (aal3v1)		10	-24	32	0.483	0.001	3.868	3.703	0.000	0.806	32	0.438
Occipital_Mid_L (aal3v1)		-30	-76	4	0.636	0.002	3.713	3.566	0.000	0.865	21	0.537
Supp_Motor_Area_R (aal3v1)	6	14	8	56	0.676	0.002	3.672	3.529	0.000	0.745	43	0.366
Frontal_Sup_2_R (aal3v1)		16	-10	60	0.693	0.002	3.654	3.513	0.000	0.740	44	0.361
Frontal_Sup_2_R (aal3v1)		14	32	46	0.745	0.002	3.599	3.463	0.000	0.762	40	0.384
Lingual_L (aal3v1)	18	-14	-78	0	0.750	0.002	3.593	3.458	0.000	0.681	55	0.306
SupraMarginal_R (aal3v1)		52	-26	24	0.810	0.003	3.523	3.395	0.000	0.871	20	0.547
Temporal_Pole_Mid_L (aal3v1)		-48	10	-28	0.000	0.001	-6.319	5.711	0.000	0.010	616	0.003
Temporal_Mid_L (aal3v1)		-56	-2	-20	0.002	0.002	-5.569	5.132	0.000			
Temporal_Mid_L (aal3v1)		-60	-8	-12	0.003	0.002	-5.480	5.061	0.000			
Insula_L (aal3v1)		-40	4	-2	0.691	0.089	-3.656	3.515	0.000	0.806	32	0.438
Right MTLE vs Control												
Temporal_Sup_L (aal3v1)		-52	-42	12	0.000	0.000	6.629	5.908	0.000	0.000	36583	0.000
ParaHippocampal_L (aal3v1)	36	-28	-14	-28	0.000	0.000	6.161	5.562	0.000			
Frontal_Inf_Orb_2_L (aal3v1)		-40	36	-8	0.000	0.000	6.062	5.488	0.000			
Supp_Motor_Area_R (aal3v1)		8	-24	58	0.015	0.000	5.115	4.747	0.000	0.001	952	0.000

K_E, cluster size; FDR, false discovery rate; FWE, family wise error; MTLE, mesial temporal lobe epilepsy; NTLE, neocortical temporal lobe epilepsy.

Region	Brodmann Area	Coordinates(mm)			Peak level					Cluster level		
		X	Y	Z	p(FWE-corr)	p(FDR-corr)	T	Z	p(unc)	p(FWE-corr)	K_E	p(unc)
Right Medial Frontal Gyrus		18	-10	54	0.022	0.000	4.988	4.644	0.000			
Supp_Motor_Area_R (aal3v1)	6	12	8	54	0.187	0.000	4.305	4.073	0.000			
Right Precentral Gyrus	6	50	-4	22	0.041	0.000	4.804	4.493	0.000	0.054	355	0.014
Postcentral_R (aal3v1)		50	-12	28	0.148	0.000	4.387	4.143	0.000			
Right Frontal Lobe/Sub-Gyral		34	0	24	0.640	0.001	3.748	3.588	0.000			
Frontal_Sup_2_R (aal3v1)		14	30	44	0.069	0.000	4.643	4.359	0.000	0.005	707	0.001
Cingulate_Mid_R (aal3v1)		10	44	30	0.081	0.000	4.589	4.314	0.000			
Right Cingulate Gyrus		18	20	34	0.652	0.001	3.737	3.578	0.000			
Parietal_Sup_R (aal3v1)		18	-66	50	0.082	0.000	4.587	4.312	0.000	0.092	288	0.024
Right Precuneus		16	-54	44	0.132	0.000	4.429	4.178	0.000			
Cingulate_Mid_L (aal3v1)		-6	-28	36	0.365	0.001	4.039	3.844	0.000	0.596	73	0.224
Cingulate_Mid_R (aal3v1)		10	-30	34	0.446	0.001	3.947	3.764	0.000	0.695	54	0.295
Frontal_Inf_Oper_R (aal3v1)		30	8	34	0.466	0.001	3.926	3.745	0.000	0.460	103	0.153
Frontal_Mid_2_R (aal3v1)		38	16	38	0.654	0.001	3.735	3.577	0.000			
Frontal_Mid_2_R (aal3v1)	9	36	32	34	0.521	0.001	3.869	3.695	0.000	0.701	53	0.299
Cingulate_Mid_L (aal3v1)	32	-2	12	40	0.864	0.002	3.490	3.358	0.000	0.818	32	0.422
Calcarine_R (aal3v1)	18	18	-86	16	0.893	0.002	3.444	3.317	0.000	0.795	36	0.394
Cuneus_R (aal3v1)		14	-80	22	0.929	0.003	3.374	3.254	0.001			
Temporal_Inf_R (aal3v1)		38	6	-42	0.000	0.000	-7.042	6.201	0.000	0.000	1515	0.000
Temporal_Pole_Mid_R (aal3v1)		42	16	-32	0.000	0.000	-6.610	5.894	0.000			
Temporal_Inf_R (aal3v1)	20	46	-4	-40	0.001	0.000	-5.952	5.405	0.000			
Insula_R (aal3v1)		40	-8	-6	0.235	0.008	-4.219	3.999	0.000	0.690	55	0.290
Left NTLE vs Control												
Right Superior Temporal Gyrus		38	-32	8	0.140	0.134	4.410	4.113	0.000	0.159	245	0.051
Right Extra-Nuclear		38	-28	-2	0.339	0.134	4.059	3.821	0.000			
Left Extra-Nuclear		-22	-6	18	0.274	0.134	4.150	3.897	0.000	0.213	206	0.071
Left Extra-Nuclear		-22	-18	16	0.505	0.134	3.863	3.654	0.000			

K_E, cluster size; FDR, false discovery rate; FWE, family wise error; MTLE, mesial temporal lobe epilepsy; NTLE, neocortical temporal lobe epilepsy.

Region	Brodmann Area	Coordinates(mm)			Peak level					Cluster level		
		X	Y	Z	p(FWE-corr)	p(FDR-corr)	T	Z	p(unc)	p(FWE-corr)	K_E	p(unc)
Thal_VPL_L (aal3v1)		-20	-22	6	0.680	0.134	3.677	3.494	0.000			
Left Frontal Lobe		-18	-22	46	0.430	0.134	3.947	3.726	0.000	0.526	89	0.220
Supp_Motor_Area_R (aal3v1)		10	-24	56	0.433	0.134	3.944	3.723	0.000	0.768	37	0.430
Right Cerebellum Anterior Lobe		14	-48	-30	0.468	0.134	3.904	3.689	0.000	0.737	43	0.394
Right Cerebellum Anterior Lobe		24	-52	-34	0.921	0.134	3.348	3.206	0.001			
Right Frontal Lobe		20	-18	46	0.476	0.134	3.895	3.682	0.000	0.757	39	0.418
Right Extra-Nuclear		28	-12	18	0.635	0.134	3.725	3.536	0.000	0.222	201	0.074
Right Extra-Nuclear		22	-18	2	0.794	0.134	3.546	3.380	0.000			
Right Extra-Nuclear		24	6	18	0.854	0.134	3.464	3.308	0.000			
Right Medial Frontal Gyrus		14	34	-10	0.724	0.134	3.629	3.453	0.000	0.727	45	0.383
Right Frontal Lobe		22	30	-6	0.931	0.134	3.324	3.184	0.001			
Right Middle Occipital Gyrus		30	-72	6	0.780	0.134	3.564	3.396	0.000	0.757	39	0.418
Calcarine_R (aal3v1)		22	-76	4	0.938	0.134	3.308	3.170	0.001			
Cerebellum_4_5_R (aal3v1)		12	-46	-4	0.875	0.134	3.433	3.281	0.001	0.804	30	0.480
Temporal_Mid_L (aal3v1)		-62	-36	-10	0.004	0.007	-5.571	5.025	0.000	0.014	615	0.004
Temporal_Mid_L (aal3v1)	21	-62	-20	-6	0.004	0.007	-5.564	5.020	0.000			
Temporal_Mid_L (aal3v1)		-60	-20	-22	0.057	0.012	-4.721	4.366	0.000			
Angular_L (aal3v1)		-52	-60	28	0.062	0.013	-4.695	4.345	0.000	0.195	218	0.064
Temporal_Mid_L (aal3v1)		-54	-56	16	0.631	0.061	-3.730	3.540	0.000			
Parietal_Inf_L (aal3v1)		-32	-60	50	0.367	0.039	-4.022	3.789	0.000	0.288	167	0.100
Right NTLE vs Control												
Cerebellum_8_L (aal3v1)		-34	-42	-44	0.737	0.199	3.686	3.473	0.000	0.320	149	0.104
Cerebellum_6_L (aal3v1)		-36	-44	-28	0.901	0.199	3.455	3.275	0.001			
Cerebellum_4_5_L (aal3v1)		-30	-36	-30	0.913	0.199	3.431	3.255	0.001			
Left Medial Frontal Gyrus		-18	52	-2	0.796	0.199	3.615	3.412	0.000	0.824	29	0.468
Cerebellum_6_L (aal3v1)		-12	-66	-12	0.799	0.199	3.610	3.408	0.000	0.144	247	0.042
Cerebellum_4_5_L (aal3v1)		-6	-46	0	0.877	0.199	3.497	3.311	0.000			

K_E, cluster size; FDR, false discovery rate; FWE, family wise error; MTLE, mesial temporal lobe epilepsy; NTLE, neocortical temporal lobe epilepsy.

Region	Brodmann Area	Coordinates(mm)			Peak level					Cluster level		
		X	Y	Z	p(FWE-corr)	p(FDR-corr)	T	Z	p(unc)	p(FWE-corr)	K_E	p(unc)
Cerebellum_6_L (aal3v1)		-14	-74	-16	0.925	0.199	3.406	3.233	0.001			
Thal_LGN_L (aal3v1)		-22	-24	-4	0.840	0.199	3.554	3.361	0.000	0.802	33	0.437
Temporal_Mid_R (aal3v1)		64	-32	-2	0.010	0.016	-5.414	4.834	0.000	0.000	1812	0.000
Temporal_Mid_R (aal3v1)	21	62	-46	0	0.042	0.016	-4.932	4.475	0.000			
Temporal_Inf_R (aal3v1)		60	-20	-26	0.045	0.016	-4.913	4.461	0.000			
Precentral_R (aal3v1)		54	-10	40	0.442	0.026	-4.014	3.746	0.000	0.509	93	0.192
Postcentral_R (aal3v1)		60	-14	36	0.772	0.044	-3.645	3.438	0.000			
Precentral_R (aal3v1)		48	6	44	0.661	0.036	-3.772	3.545	0.000	0.792	35	0.423
Frontal_Sup_2_R (aal3v1)		22	-6	70	0.738	0.041	-3.686	3.472	0.000	0.861	22	0.532

K_E, cluster size; FDR, false discovery rate; FWE, family wise error; MTLE, mesial temporal lobe epilepsy; NTLE, neocortical temporal lobe epilepsy.

Metabolic abnormalities in patients with NTLE

Similarly, the epileptogenic regions of NTLE group were also well-lateralized to the left NTLE (n = 28) and right NTLE (n = 18). In addition to ipsilateral temporal lobe, the patients with NTLE showed hypometabolism in the ipsilateral frontal lobe and parietal lobe ($p < 0.001$, uncorrected). When it comes to regional cerebral hypermetabolism, the hypermetabolism in the brain with NTLE was limited to contralateral temporal lobe and cerebellum, ipsilateral frontal, occipital lobe, insula, and bilateral thalamus ($p < 0.001$, uncorrected). The render and slice view of NTLE compared with HC were shown in Fig. 2. Interestingly, different from MTLE, hypermetabolism was observed only in contralateral cerebellum.

The volume of hypermetabolism in temporal and extratemporal regions

Significant differences were found in the metabolic patterns of MTLE and NTLE, especially in the hypermetabolic regions. Figure 3 demonstrated the involved volume of metabolic abnormality in patients with MTLE compared to patients with NTLE. In both right and left TLE, MTLE patients had significantly higher hypermetabolic volumes in each of these regions than NTLE patients, including contralateral temporal lobe and frontal, parietal, occipital lobe, insula, limbic lobe, basal ganglia, thalamus, brainstem, and cerebellum. The difference in hypermetabolism between the two types of right TLEs is greater than the left TLE. Additionally, the hypometabolic region of MTLE involved only the temporal lobe and insula, while the hypometabolic regions of left NTLE involved the temporal and parietal lobes, and right NTLE involved the temporal, parietal, and frontal lobes.

The correlation between surgical outcome and abnormal metabolic volume of specific extratemporal brain regions

Based on available clinical data including detailed neurologic history, physical examination, MRI, video EEG or SEEG, and joint decision of MDT, 76 MTLE patients (83.5%) and 23 NTLE patients (50%) underwent epilepsy surgery. Seventy-five patients with MTLE went through anterior temporal lobectomy and remaining patient with MTLE was operated with target destruction. All patients with NTLE underwent tailored resection of the lateral temporal neocortex. Except for one patient who underwent target destruction, postoperative pathology was done in 98 patients (Table 3). With an average follow-up of 2.9 years after surgery, 61 of 99 patients achieved an Engel class IA outcome. Seizure-free were more frequently achieved in MTLE patients than in NTLE patients (67.1% vs 43.5%, $p = 0.041$). Furthermore, we divided the two groups into Engel class IA representing good surgical outcomes and non-Engel class IA for volume comparison. In the MTLE group, the hypermetabolic volumes for the frontal lobe and thalamus were larger in non-Engel class IA patients than in Engel class IA patients ($p < 0.05$), while no other significantly different hyper- and hypo- metabolic regions were found between the non-Engel class IA and Engel class IA patients. In the NTLE group, there was no statistical difference between the hyper- and hypo- metabolic regions in the patients with different surgical outcomes (Table 4).

Table 3
Surgical data of patients who underwent surgery

	MTLE(n = 76)	NTLE(n = 23)	P value
Surgical approach, n (%)			
Anterior temporal lobectomy	75 (98.7%)	0 (0.0%)	NA
Tailored resection of the lateral temporal neocortex	0 (0.0%)	23 (100.0%)	
Target destruction	1 (1.3%)	0 (0.0%)	
Postoperative pathology			
HS, n (%)	33(44.0%)	0(0.0%)	NA
FCD, n (%)	11(14.7%)	7(30.4%)	
Gliosis, n (%)	25(33.3%)	6(26.1%)	
Tumor, n (%)	2(2.7%)	3(13.0%)	
Other, n (%)	4(5.3%)	7(30.4%)	
Surgical outcomes			
Engel class IA, n (%)	51(67.1)	10(43.5%)	0.041#,*
Non-Engel class IA, n (%)	25(32.9%)	13(56.5%)	

Chi-square test or Fisher Exact test

* Bold values indicate significant difference (P < 0.05)

FCD, focal cortical dysplasia; HS, hippocampal sclerosis; MTLE, mesial temporal lobe epilepsy; NA not application; NTLE, neocortical temporal lobe epilepsy.

Table 4
Significant change in glucose metabolism involving different cerebral regions in patients with MTLE or NTLE with different surgical outcomes.

	MTLE(n = 76)		P value	NTLE(n = 23)		P value
	Engel class IA n = 51	Non-Engel class IA n = 25		Engel class IA n = 10	Non-Engel class IA n = 13	
The volume of metabolic increase, median (IQR)						
Temporal lobe	4 (0-105)	40 (0-190)	0.351ε	0 (0-125)	0 (0-62.5)	0.597ε
Frontal lobe	30 (0-128)	73 (14.5–331)	**0.027ε,***	25 (0-955)	0 (0-315)	0.493ε
Parietal lobe	1 (0-146)	66 (0-222)	0.107ε	0 (0-317.75)	0 (0-49.5)	0.805ε
Occipital lobe	0 (0–40)	0(0-46.5)	0.466ε	0 (0-131.5)	0 (0-70.5)	0.827ε
Insula	0 (0–6)	0 (0–22)	0.324ε	0 (0-7.5)	0 (0–13)	0.970ε
Limbic system	0 (0–37)	16 (0-85.5)	0.254ε	6 (0-112)	0 (0-172.5)	0.632ε
Basal ganglia	0 (0–23)	5 (0–81)	0.199ε	0 (0-30.5)	0 (0-23.5)	0.970ε
Thalamus	0 (0–0)	0 (0–35)	**0.019ε,***	0 (0–0)	0 (0–0)	0.791ε
Brainstem	0 (0–0)	0 (0–0)	0.177ε	0 (0–0)	0 (0–0)	0.177ε
Cerebellum	0 (0–31)	0 (0–81)	0.756ε	0 (0-107.25)	0 (0-39.5)	0.610ε
The volume of metabolic decrease, median (IQR)						
Temporal lobe	22 (0-163)	54 (0-597.5)	0.273ε	186 (0-651)	18 (0-583)	0.660ε
Frontal lobe	0 (0–24)	0 (0–55)	0.876ε	192.5 (0-519)	0 (0-150.5)	**0.113ε,***
Parietal lobe	0 (0–23)	0 (0-10.5)	0.902ε	10.5 (0-833.5)	42 (0-125.5)	0.942ε
Occipital lobe	0 (0–0)	0 (0–0)	0.237ε	0 (0-670)	0 (0–22)	0.942ε
Insula	0 (0–0)	0 (0–0)	0.072ε	0 (0–36)	0 (0–0)	0.335ε
Limbic system	0 (0–0)	0 (0–0)	0.197ε	0 (0-292)	0 (0-7.5)	0.286ε
Basal ganglia	0 (0–0)	0 (0–0)	0.590ε	0 (0–8)	0 (0-1.5)	0.630ε
Thalamus	NA	NA	NA	NA	NA	NA
Brainstem	0 (0–0)	0 (0–0)	0.484ε	NA	NA	NA
Cerebellum	0 (0–0)	0 (0–0)	0.493ε	0 (0-69.75)	0 (0–0)	0.323ε

ε Mann-Whitney *U* test

* Bold values indicate significant difference (P < 0.05)

MTLE, mesial temporal lobe epilepsy; NA not application; NTLE, neocortical temporal lobe epilepsy.

Discussion

In our study using whole-brain voxel-based ^{18}F-FDG-PET, a striking difference in metabolic patterns between MTLE and NTLE was observed. Patients with MTLE displayed a characteristic ipsilateral hypometabolism in the temporal lobe and bilateral cortical-subcortical

hypermetabolism pattern. In contrast, NTLE patients showed more extensive hypometabolic regions including the temporal and front-parietal cortex, and hypermetabolic in certain cortical regions. The difference in metabolic patterns between the two TLE subtypes may represent distinct epileptic networks that can guide the clinical classification of epilepsy. Hypometabolism involving ipsilateral thalamus and bilateral frontal lobe could be a predictor of an unfavorable seizure outcome in TLE, which could facilitate preoperative counseling and surgical planning.

^{18}F-FDG-PET has been widely used in patients with medically refractory focal epilepsy for detection of the epileptogenic lesion[11, 14, 15]. Pathologic reduction in glucose metabolism indicates focal neuronal and synaptic loss associated with epileptogenic brain region[24]. Our study has identified two patterns of cerebral hypometabolism in the MTLE and NTLE groups. Glucose hypometabolism of metabolism is present in ipsilateral hippocampus and insular lobe in MTLE. It is well accepted that the medial structure of the temporal lobe including hippocampus is the seizure origination location in MTLE, and as spikes propagate, the cortical insula commonly becomes the earliest involved structure via the Papez circuit. Recurrent spike distribution and seizure propagation from mesial temporal lobe to insular cortex contribute to focal metabolic impairment in insular, or even lead to insular atrophy[25]·[26]. In NTLE, the hypometabolic region is mainly located in the temporal neocortex associated with EZ. Notably, we have also found some restricted extratemporal cortical regions in frontal and parietal lobes showing decreased glucose metabolism in NTLE patients, suggesting more extensive brain regions and connected propagated networks affected in NTLE. Therefore, it is plausible that patients with NTLE usually demonstrate behavioral arrest with awareness impairment at the early stage[27, 28] and followed with motor signs as the seizure activity spread to the frontoparietal convexity[29–31].

A more significant disparity in hypermetabolic patterns is found between MTLE and NTLE patients. Both showed hypermetabolism in cortical and subcortical regions but with different locations. Glucose metabolism is commonly enhanced in the bilateral basal ganglia, brainstem, thalamus, corpus callosum, cingulate gyrus, and frontoparietal-occipital cortex, suggesting the propagation pathway in these structures probably be involved in the MTLE group[32–36]. The thalamus and brainstem are distinctly connected with the cingulate gyrus and cerebral cortex[37, 38]. A focal seizure that originates from the mesial structure of temporal lobe usually spreads to key subcortical regions such as the brainstem and bilateral thalamus, resulting in widespread metabolic disturbance in midline subcortical structures and neocortex[39–42]. Additionally, large areas of hypermetabolism in contralateral cerebral regions of MTLE seem to result from the restoration of chemical homeostasis[43].

Although cortical and subcortical hypermetabolism extra the EZ is also present among the patient with NTLE, it is much more restricted in the range of glucose metabolism. Notably, the key hypermetabolic region of NTLE is typically bilateral thalamus, suggestive of an underlying propagation pathway from the lateral neocortex of temporal lobe through the basal ganglia to the contralateral hemisphere that contributes to bilateral tonic-clonic seizures[44]. Considering the extent of involvement, we speculate that except for the trans-thalamic circuits, other propagating pathways may exist in NTLE[45].

In addition, we observed significant hypermetabolism in the cerebellar, consistent with previous functional MRI and SPECT studies[46, 47]. Sufficient data indicate that cerebellum is engaged during seizures, manifesting as reduced gray matter volumes[48] and an increased cerebellar blood flow and neuronal activities during seizures[49, 50]. Experimentally, increased interictal metabolic activities in the cerebellum have also been reported in animal models of epilepsy[51]. The cerebellar metabolic changes in TLE patients in our study suggest a functional significance of temporal-cerebellar connections and the potential ability for cerebellar activation to inhibit seizures[52]. Another possibility is that the abnormal glucose metabolism in the cerebellum may be compensatory as one of the downstream targets through divergent output pathways from temporal lobe[50]. Of interest, bilateral cerebellum is likely to be affected in MTLE, while abnormal metabolism is only found in the contralateral cerebellar hemisphere in the NTLE group, highlighting the potential importance of the cerebellum in differentiation of epilepsy phenotypes in TLE.

We have further assessed metabolic features and surgical outcomes in patients with two subtypes of TLE. We find that patients with MTLE have a worse surgical prognosis if thalamic or frontal hypermetabolism is present. Lesional mesial temporal lobe epilepsy usually include hippocampal sclerosis, focal cortical dysplasia, or local neurodevelopmental tumors[53, 54]. Due to their limited focal damages, standard anterior temporal lobectomy offers comparatively favorable outcomes (50–80% seizure-free rate)[55, 56]. However, if combined with an extended frontal or thalamic ^{18}F-FDG metabolic disturbance, actual lesions associated with epileptogenesis or seizure related networks in MTLE may be larger than they appear on structural imaging. As a result, the removal of only the anterior temporal lobe region may not be sufficient for postsurgical seizure control. For this reason, surgical procedure selection should be comprehensively determined if MTLE patients show thalamic or frontal involvement on the ^{18}F-FDG-PET images. Precise and sufficient location of epileptogenic foci, including invasive EEG, should be carefully carried out for better surgical outcomes.

Several limitations in our study should be mentioned. This is a retrospective study, which inevitably brings selection biases. The sample size is relatively small, especially for the NTLE group that only accounts for 10% of TLE[57]. Even though ASMs were discontinued for at least 24 h before the PET scan, they may still have residual effects on brain metabolism, which should be avoided in future studies. The decision to undergo a resection procedure is complex involving consideration of the patients' preoperative structural MRI, video-EEG, and invasive SEEG.

Conclusions

Distinctive characteristic features of ^{18}F-FDG-PET metabolic profiles have been identified in NTLE and MTLE patients. The glucose hypometabolism is associated with EZ, while the hypermetabolic regions suggest their different propagation networks and underlying compensatory mechanism. Importantly, the presence of hypermetabolism involving thalamus and frontal lobe in MTLE may be a predictor of larger epileptogenic foci and an unfavorable seizure surgical outcome. Comprehensive evaluations including invasive EEG should be applied in clinical practice.

Declarations

Acknowledgements We would like to express gratitude to all the patients with temporal lobe epilepsy for their cooperation in our study. We would also like to thank the researchers for their contributions in collecting and following up with the patients.

Author contribution All authors contributed to the study conception and design. Material preparation, data collection, and analysis were performed by Haoyue Zhu, Yongxiang Tang, Ling Xiao, Shirui Wen, Yuanxia Wu, Zhiquan Yang, Luo Zhou and Bo Xiao. The first draft of the manuscript was written by Haoyue Zhu and Li Feng. Li Feng and Shuo Hu revised the work critically for important intellectual content. All authors commented on previous versions of the manuscript. All authors read and approved the fnal manuscript.

Funding This work was supported by the following funding source: National Natural Science Foundation of China (No. 91859207, 82071461 and 81801740), Hunan Provincial Natural Science Foundation of China (No. 2021JJ31060 and 2020JJ5922), and Innovative Construction Foundation of Hunan Province, (No. 2021SK4001).

Data availability The datasets generated and/or analyzed during the current study are available from the corresponding author on reasonable request.

Code availability Not applicable

Ethics approval We confirm that we have read Journal's position on issues involved in ethical publication and affirm that this study is consistent with those guidelines. The ethics committee of Xiangya Hospital approved the protocol before patient recruitment commenced. The procidures used in this study adhere to the tenets of the Declaration of Helsinki.

Consent for participate All individual participants or legal guardians signed written informed consent before participation in the study.

Consent to publish Patients signed informed consent regarding the publication of their data and photographs.

Conflict of interest The authors declare no competing interests.

References

1. Abarrategui B, Mai R, Sartori I, Francione S, Pelliccia V, Cossu M, et al. Temporal lobe epilepsy: A never-ending story. Epilepsy Behav. 2021;122:108122. doi:10.1016/j.yebeh.2021.108122.
2. Proposal for revised classification of epilepsies and epileptic syndromes. Commission on Classification and Terminology of the International League Against Epilepsy. Epilepsia. 1989;30:389–99. doi:10.1111/j.1528-1157.1989.tb05316.x.
3. Janszky J, Pannek HW, Fogarasi A, Bone B, Schulz R, Behne F, et al. Prognostic factors for surgery of neocortical temporal lobe epilepsy. Seizure. 2006;15:125–32. doi:10.1016/j.seizure.2005.12.002.
4. Foldvary N, Lee N, Thwaites G, Mascha E, Hammel J, Kim H, et al. Clinical and electrographic manifestations of lesional neocortical temporal lobe epilepsy. Neurology. 1997;49:757–63. doi:10.1212/wnl.49.3.757.
5. Madhavan D, Kuzniecky R. Temporal lobe surgery in patients with normal MRI. Curr Opin Neurol. 2007;20:203–7. doi:10.1097/WCO.0b013e328042baba.
6. Maillard L, Vignal JP, Gavaret M, Guye M, Biraben A, McGonigal A, et al. Semiologic and electrophysiologic correlations in temporal lobe seizure subtypes. Epilepsia. 2004;45:1590–9. doi:10.1111/j.0013-9580.2004.09704.x.
7. Schulz R, Lüders HO, Hoppe M, Tuxhorn I, May T, Ebner A. Interictal EEG and ictal scalp EEG propagation are highly predictive of surgical outcome in mesial temporal lobe epilepsy. Epilepsia. 2000;41:564–70. doi:10.1111/j.1528-1157.2000.tb00210.x.
8. Wang YH, An Y, Fan XT, Lu J, Ren LK, Wei PH, et al. Comparison between simultaneously acquired arterial spin labeling and (18)F-FDG PET in mesial temporal lobe epilepsy assisted by a PET/MR system and SEEG. Neuroimage Clin. 2018;19:824–30. doi:10.1016/j.nicl.2018.06.008.

9. Duncan JS, Winston GP, Koepp MJ, Ourselin S. Brain imaging in the assessment for epilepsy surgery. Lancet Neurol. 2016;15:420–33. doi:10.1016/S1474-4422(15)00383-X.
10. Guedj E, Bonini F, Gavaret M, Trebuchon A, Aubert S, Boucekine M, et al. (18)FDG-PET in different subtypes of temporal lobe epilepsy: SEEG validation and predictive value. Epilepsia. 2015;56:414–21. doi:10.1111/epi.12917.
11. von Oertzen TJ. PET and ictal SPECT can be helpful for localizing epileptic foci. Curr Opin Neurol. 2018;31:184–91. doi:10.1097/WCO.0000000000000527.
12. Chassoux F, Rodrigo S, Semah F, Beuvon F, Landre E, Devaux B, et al. FDG-PET improves surgical outcome in negative MRI Taylor-type focal cortical dysplasias. Neurology. 2010;75:2168–75. doi:10.1212/WNL.0b013e31820203a9.
13. Kikuchi K, Togao O, Yamashita K, Momosaka D, Nakayama T, Kitamura Y, et al. Diagnostic accuracy for the epileptogenic zone detection in focal epilepsy could be higher in FDG-PET/MRI than in FDG-PET/CT. Eur Radiol. 2021;31:2915–22. doi:10.1007/s00330-020-07389-1.
14. Duncan JS, Winston GP, Koepp MJ, Ourselin S. Brain imaging in the assessment for epilepsy surgery. Lancet Neurol. 2016;15:420–33. doi:10.1016/s1474-4422(15)00383-x.
15. Jaisani Z, Miletich RS, Ramanathan M, Weinstock AL. Clinical FDG-PET Findings in Patients with Temporal Lobe Epilepsy: Concordance with EEG and MRI. J Neuroimaging. 2020;30:119–25. doi:10.1111/jon.12671.
16. Riederer I, Bohn KP, Preibisch C, Wiedemann E, Zimmer C, Alexopoulos P, et al. Alzheimer Disease and Mild Cognitive Impairment: Integrated Pulsed Arterial Spin-Labeling MRI and (18)F-FDG PET. Radiology. 2018;288:198–206. doi:10.1148/radiol.2018170575.
17. Diehl J, Grimmer T, Drzezga A, Riemenschneider M, Förstl H, Kurz A. Cerebral metabolic patterns at early stages of frontotemporal dementia and semantic dementia. A PET study. Neurobiol Aging. 2004;25:1051–6. doi:10.1016/j.neurobiolaging.2003.10.007.
18. Fisher RS, Cross JH, French JA, Higurashi N, Hirsch E, Jansen FE, et al. Operational classification of seizure types by the International League Against Epilepsy: Position Paper of the ILAE Commission for Classification and Terminology. Epilepsia. 2017;58:522–30. doi:10.1111/epi.13670.
19. Scheffer IE, Berkovic S, Capovilla G, Connolly MB, French J, Guilhoto L, et al. ILAE classification of the epilepsies: Position paper of the ILAE Commission for Classification and Terminology. Epilepsia. 2017;58:512–21. doi:10.1111/epi.13709.
20. Engel J Jr, Wiebe S, French J, Sperling M, Williamson P, Spencer D, et al. Practice parameter: temporal lobe and localized neocortical resections for epilepsy: report of the Quality Standards Subcommittee of the American Academy of Neurology, in association with the American Epilepsy Society and the American Association of Neurological Surgeons. Neurology. 2003;60:538–47. doi:10.1212/01.wnl.0000055086.35806.2d.
21. Barot N, Batra K, Zhang J, Klem ML, Castellano J, Gonzalez-Martinez J, et al. Surgical outcomes between temporal, extratemporal epilepsies and hypothalamic hamartoma: systematic review and meta-analysis of MRI-guided laser interstitial thermal therapy for drug-resistant epilepsy. J Neurol Neurosurg Psychiatry. 2022;93:133–43. doi:10.1136/jnnp-2021-326185.
22. Varrone A, Asenbaum S, Vander Borght T, Booij J, Nobili F, Någren K, et al. EANM procedure guidelines for PET brain imaging using [18F]FDG, version 2. Eur J Nucl Med Mol Imaging. 2009;36:2103–10. doi:10.1007/s00259-009-1264-0.
23. Tang Y, Liow JS, Zhang Z, Li J, Long T, Li Y, et al. The Evaluation of Dynamic FDG-PET for Detecting Epileptic Foci and Analyzing Reduced Glucose Phosphorylation in Refractory Epilepsy. Front NeuroSci. 2018;12:993. doi:10.3389/fnins.2018.00993.
24. Blazhenets G, Schroeter N, Bormann T, Thurow J, Wagner D, Frings L, et al. Slow but Evident Recovery from Neocortical Dysfunction and Cognitive Impairment in a Series of Chronic COVID-19 Patients. J Nucl Med. 2021;62:910–5. doi:10.2967/jnumed.121.262128.
25. Isnard J, Guénot M, Ostrowsky K, Sindou M, Mauguière F. The role of the insular cortex in temporal lobe epilepsy. Ann Neurol. 2000;48:614–23.
26. Jupp B, Williams J, Binns D, Hicks RJ, Cardamone L, Jones N, et al. Hypometabolism precedes limbic atrophy and spontaneous recurrent seizures in a rat model of TLE. Epilepsia. 2012;53:1233–44. doi:10.1111/j.1528-1167.2012.03525.x.
27. Englot DJ, Hinkley LB, Kort NS, Imber BS, Mizuiri D, Honma SM, et al. Global and regional functional connectivity maps of neural oscillations in focal epilepsy. Brain. 2015;138:2249–62. doi:10.1093/brain/awv130.
28. Englot DJ, Yang L, Hamid H, Danielson N, Bai X, Marfeo A, et al. Impaired consciousness in temporal lobe seizures: role of cortical slow activity. Brain. 2010;133:3764–77. doi:10.1093/brain/awq316.
29. Bone B, Fogarasi A, Schulz R, Gyimesi C, Kalmar Z, Kovacs N, et al. Secondarily generalized seizures in temporal lobe epilepsy. Epilepsia. 2012;53:817–24. doi:10.1111/j.1528-1167.2012.03435.x.
30. O'Brien TJ, Kilpatrick C, Murrie V, Vogrin S, Morris K, Cook MJ. Temporal lobe epilepsy caused by mesial temporal sclerosis and temporal neocortical lesions. A clinical and electroencephalographic study of 46 pathologically proven cases. Brain. 1996;119(Pt 6):2133–41. doi:10.1093/brain/119.6.2133.
31. Foldvary-Schaefer N, Unnwongse K. Localizing and lateralizing features of auras and seizures. Epilepsy Behav. 2011;20:160–6. doi:10.1016/j.yebeh.2010.08.034.

32. Rossi LF, Wykes RC, Kullmann DM, Carandini M. Focal cortical seizures start as standing waves and propagate respecting homotopic connectivity. Nat Commun. 2017;8:217. doi:10.1038/s41467-017-00159-6.
33. Catenoix H, Magnin M, Guénot M, Isnard J, Mauguière F, Ryvlin P. Hippocampal-orbitofrontal connectivity in human: an electrical stimulation study. Clin Neurophysiol. 2005;116:1779–84. doi:10.1016/j.clinph.2005.03.016.
34. Zeng H, Pizarro R, Nair VA, La C, Prabhakaran V. Alterations in regional homogeneity of resting-state brain activity in mesial temporal lobe epilepsy. Epilepsia. 2013;54:658–66. doi:10.1111/epi.12066.
35. Wiest R, Estermann L, Scheidegger O, Rummel C, Jann K, Seeck M, et al. Widespread grey matter changes and hemodynamic correlates to interictal epileptiform discharges in pharmacoresistant mesial temporal epilepsy. J Neurol. 2013;260:1601–10. doi:10.1007/s00415-013-6841-2.
36. Lieb JP, Dasheiff RM, Engel J. Jr. Role of the frontal lobes in the propagation of mesial temporal lobe seizures. Epilepsia. 1991;32:822–37. doi:10.1111/j.1528-1157.1991.tb05539.x.
37. Feng L, Motelow JE, Ma C, Biche W, McCafferty C, Smith N, et al. Seizures and Sleep in the Thalamus: Focal Limbic Seizures Show Divergent Activity Patterns in Different Thalamic Nuclei. J Neurosci. 2017;37:11441–54. doi:10.1523/jneurosci.1011-17.2017.
38. Blumenfeld H, Varghese GI, Purcaro MJ, Motelow JE, Enev M, McNally KA, et al. Cortical and subcortical networks in human secondarily generalized tonic-clonic seizures. Brain. 2009;132:999–1012. doi:10.1093/brain/awp028.
39. Aracri P, de Curtis M, Forcaia G, Uva L. Enhanced thalamo-hippocampal synchronization during focal limbic seizures. Epilepsia. 2018;59:1774–84. doi:10.1111/epi.14521.
40. Chen B, Xu C, Wang Y, Lin W, Wang Y, Chen L, et al. A disinhibitory nigra-parafascicular pathway amplifies seizure in temporal lobe epilepsy. Nat Commun. 2020;11:923. doi:10.1038/s41467-020-14648-8.
41. Englot DJ, Gonzalez HFJ, Reynolds BB, Konrad PE, Jacobs ML, Gore JC, et al. Relating structural and functional brainstem connectivity to disease measures in epilepsy. Neurology. 2018;91:e67–77. doi:10.1212/wnl.0000000000005733.
42. Fasano A, Eliashiv D, Herman ST, Lundstrom BN, Polnerow D, Henderson JM, et al. Experience and consensus on stimulation of the anterior nucleus of thalamus for epilepsy. Epilepsia. 2021;62:2883–98. doi:10.1111/epi.17094.
43. Wu D, Yang L, Gong G, Zheng Y, Jin C, Qi L, et al. Characterizing the hyper- and hypometabolism in temporal lobe epilepsy using multivariate machine learning. J Neurosci Res. 2021;99:3035–46. doi:10.1002/jnr.24951.
44. Cui Y, Liu J, Luo Y, He S, Xia Y, Zhang Y, et al. Aberrant Connectivity During Pilocarpine-Induced Status Epilepticus. Int J Neural Syst. 2020;30:1950029. doi:10.1142/s0129065719500291.
45. Sirin NG, Yilmaz E, Bebek N, Baykan B, Gokyigit A, Gurses C. Unusual ictal propagation patterns suggesting poor prognosis after temporal lobe epilepsy surgery: Switch of lateralization and bilateral asynchrony. Epilepsy Behav. 2018;86:31–6. doi:10.1016/j.yebeh.2018.07.013.
46. Blumenfeld H, McNally KA, Vanderhill SD, Paige AL, Chung R, Davis K, et al. Positive and negative network correlations in temporal lobe epilepsy. Cereb Cortex. 2004;14:892–902.
47. Li H, Ji C, Zhu L, Huang P, Jiang B, Xu X, et al. Reorganization of anterior and posterior hippocampal networks associated with memory performance in mesial temporal lobe epilepsy. Clin Neurophysiol. 2017;128:830–8. doi:10.1016/j.clinph.2017.02.018.
48. Oyegbile TO, Bayless K, Dabbs K, Jones J, Rutecki P, Pierson R, et al. The nature and extent of cerebellar atrophy in chronic temporal lobe epilepsy. Epilepsia. 2011;52:698–706. doi:10.1111/j.1528-1167.2010.02937.x.
49. Bantli H, Bloedel JR, Tolbert D. Activation of neurons in the cerebellar nuclei and ascending reticular formation by stimulation of the cerebellar surface. J Neurosurg. 1976;45:539–54. doi:10.3171/jns.1976.45.5.0539.
50. Shin WC, Hong SB, Tae WS, Seo DW, Kim SE. Ictal hyperperfusion of cerebellum and basal ganglia in temporal lobe epilepsy: SPECT subtraction with MRI coregistration. J Nucl Med. 2001;42:853–8.
51. Folbergrová J, Ingvar M, Siesjö BK. Metabolic changes in cerebral cortex, hippocampus, and cerebellum during sustained bicuculline-induced seizures. J Neurochem. 1981;37:1228–38. doi:10.1111/j.1471-4159.1981.tb04673.x.
52. Streng ML, Krook-Magnuson E. The cerebellum and epilepsy. Epilepsy Behav. 2021;121:106909. doi:10.1016/j.yebeh.2020.106909.
53. Chassoux F, Artiges E, Semah F, Laurent A, Landré E, Turak B, et al. (18)F-FDG-PET patterns of surgical success and failure in mesial temporal lobe epilepsy. Neurology. 2017;88:1045–53. doi:10.1212/wnl.0000000000003714.
54. Lagarde S, Bonini F, McGonigal A, Chauvel P, Gavaret M, Scavarda D, et al. Seizure-onset patterns in focal cortical dysplasia and neurodevelopmental tumors: Relationship with surgical prognosis and neuropathologic subtypes. Epilepsia. 2016;57:1426–35. doi:10.1111/epi.13464.
55. Sone D, Ahmad M, Thompson PJ, Baxendale S, Vos SB, Xiao F, et al. Optimal Surgical Extent for Memory and Seizure Outcome in Temporal Lobe Epilepsy. Ann Neurol. 2022;91:131–44. doi:10.1002/ana.26266.
56. Cahill V, Sinclair B, Malpas CB, McIntosh AM, Chen Z, Vivash LE, et al. Metabolic patterns and seizure outcomes following anterior temporal lobectomy. Ann Neurol. 2019;85:241–50. doi:10.1002/ana.25405.

57. Maizuliana H, Usui N, Terada K, Kondo A, Inoue Y. Clinical, semiological, electroencephalographic, and neuropsychological features of "pure" neocortical temporal lobe epilepsy. Epileptic Disord. 2020;22:55–65. doi:10.1684/epd.2020.1132.

Figures

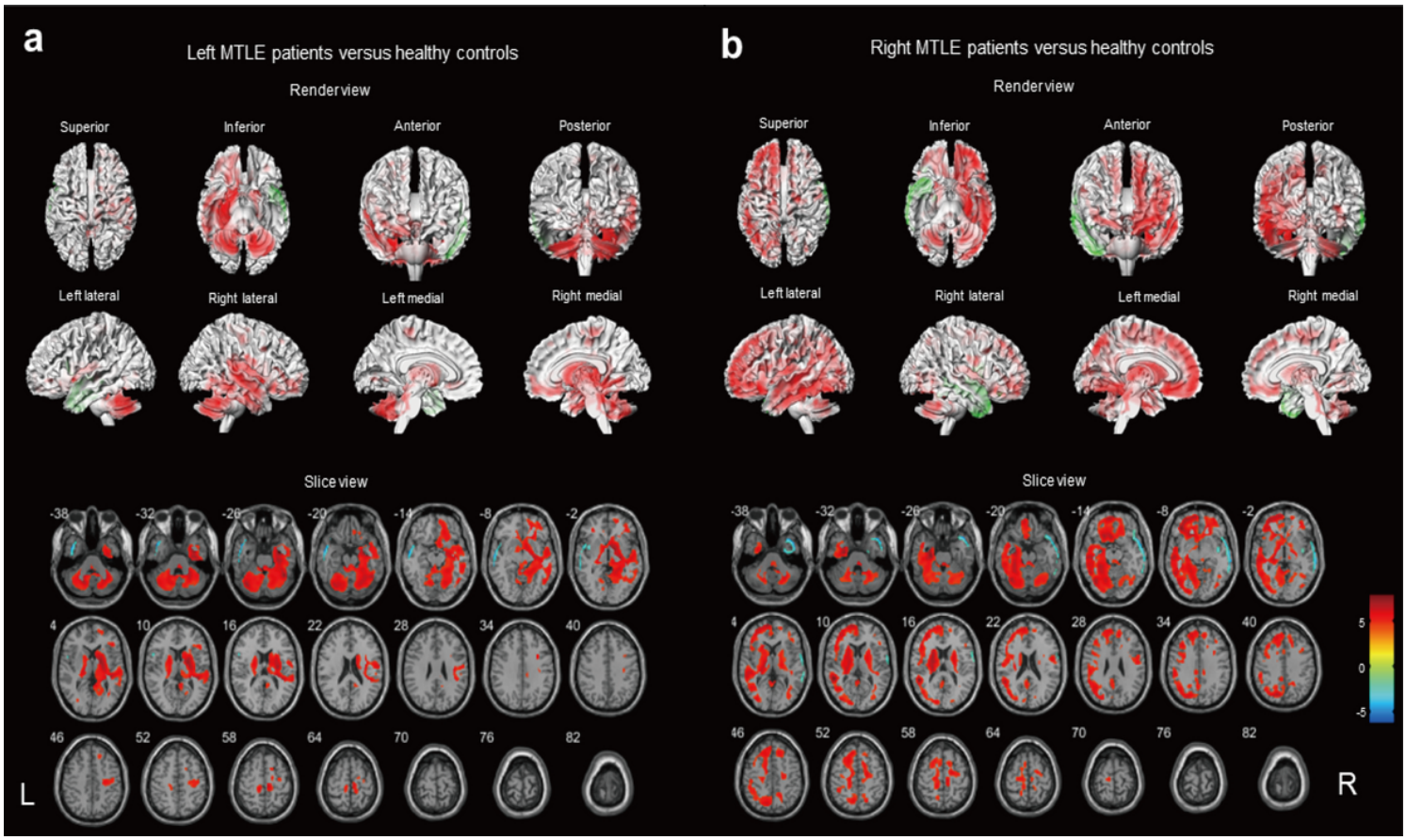

Figure 1

Comparison of patients with differed in MTLE (N=91) versus healthy controls (N = 40) ($p<0.001$, uncorrected). Voxels with significantly low uptake are shown in green and high uptake are shown in red. (a) Left MTLE patients (N=48) versus healthy controls was performed in render view (upper) and slice view (below). (b) Right MTLE patients (N=43) versus healthy controls was performed in render view (upper) and slice view (below). Abbreviation: MTLE, mesial temporal lobe epilepsy.

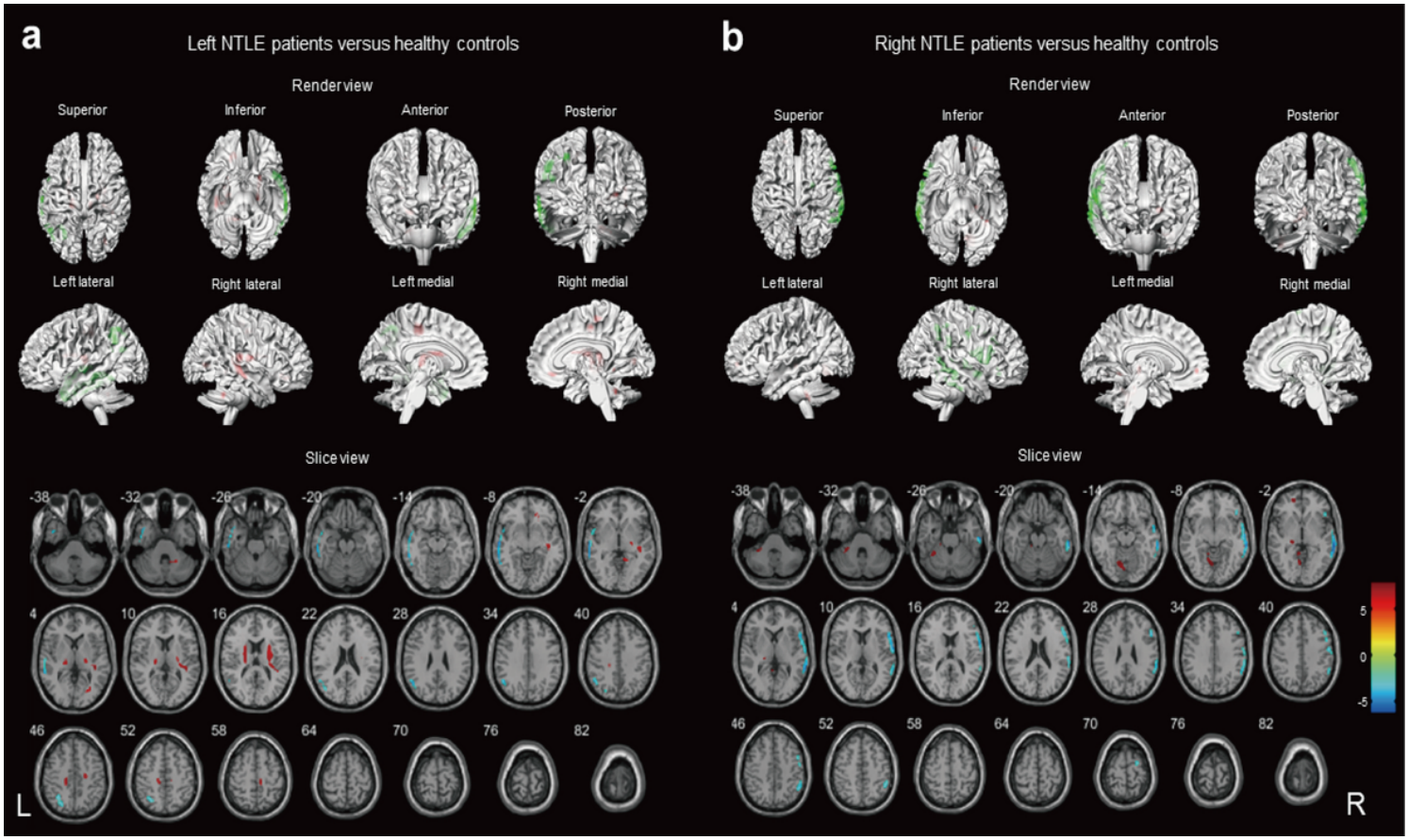

Figure 2

Comparison of patients with differed in NTLE (N=46) versus healthy controls (N = 40) ($p<0.001$, uncorrected). Voxels with significantly low uptake are shown in green and high uptake are shown in red. (a) Left NTLE patients (N=28) versus healthy controls was performed in render view (upper) and slice view (below). (b) Right NTLE patients (N=18) versus healthy controls was performed in render view (upper) and slice view (below). Abbreviation: NTLE, neocortical temporal lobe epilepsy.

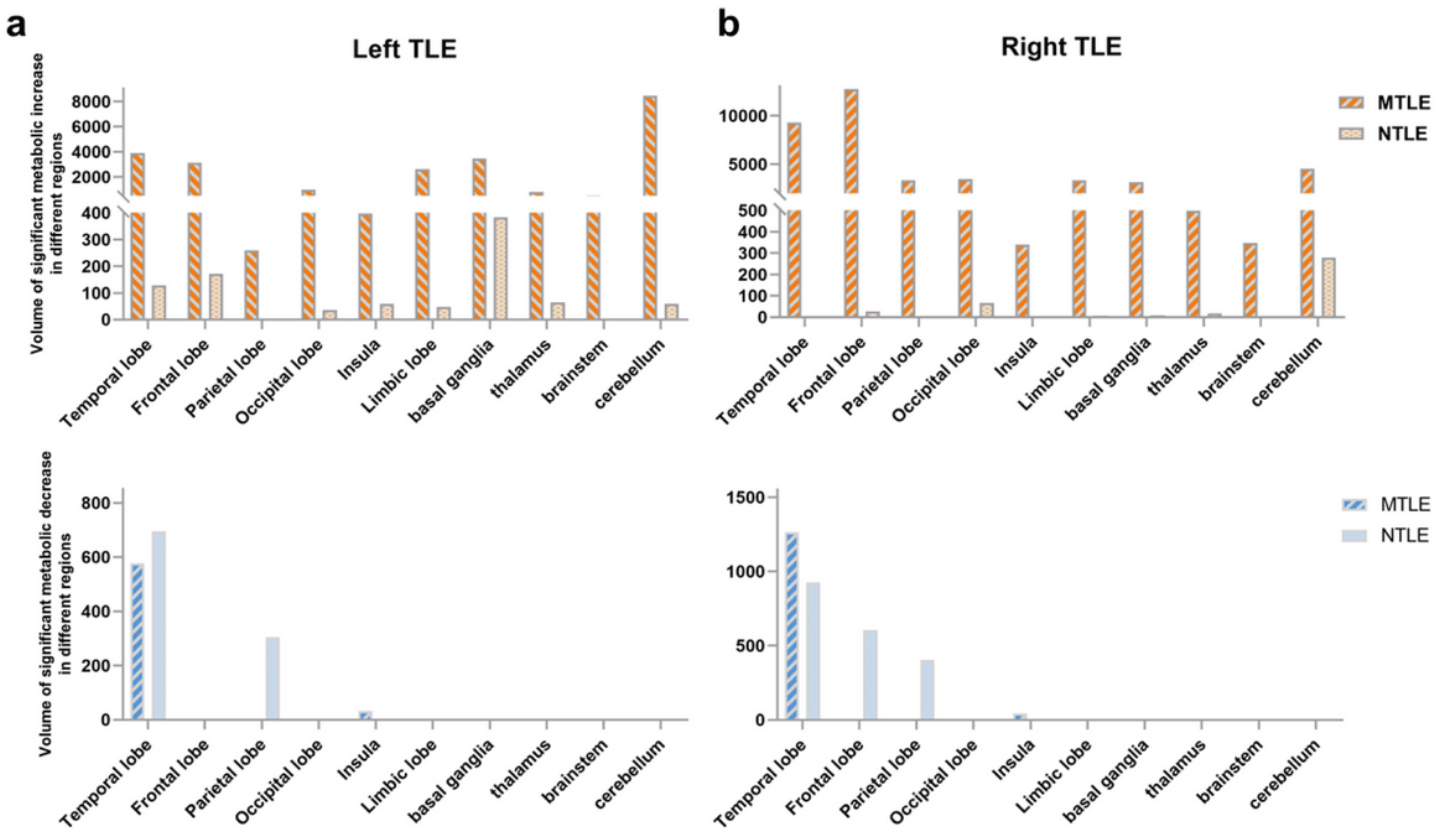

Figure 3

Involvement volume of abnormal metabolism in patients with MTLE compared to patients with NTLE. We compared the metabolic increased (upper, orange) and decreased (below, blue) volume of involvement of each cerebral region in the two groups. In both left (a) and right (b) TLE, MTLE patients had significantly higher hypermetabolic volumes in each of these regions than NTLE patients, including contralateral temporal lobe and frontal, parietal, occipital lobe, insula, limbic lobe, basal ganglia, thalamus, brainstem, and cerebellum. The difference between the two types of right TLEs is greater than the left TLE. The hypometabolic region of MTLE involves only the temporal lobe and insula, while hypometabolic region of left NTLE involved temporal and parietal lobe, as well as hypometabolic region of right NTLE involved temporal, parietal, and frontal lobe. Abbreviation: TLE, temporal lobe epilepsy; MTLE, mesial temporal lobe epilepsy; NTLE, neocortical temporal lobe epilepsy.